POLİTEKNİK DERGİSİ

JOURNAL of POLYTECHNIC

ISSN: 1302-0900 (PRINT), ISSN: 2147-9429 (ONLINE)
URL: http://dergipark.org.tr/politeknik

Finite element analyzing of the effect of crack on mechanical behavior of honeycomb and re-entrant structures

Çatlağın re-entrant ve balpeteği yapıların mekanik davranışlarına etkisinin sonlu eleman analizi

***Yazar(lar) (Author(s))**: Berkay ERGENE[1], Bekir YALÇIN[2]*

ORCID[1] : 0000-0001-6145-1970

ORCID[2] : 0000-0002-3784-7251

Bu makaleye şu şekilde atıfta bulunabilirsiniz(To cite to this article): Ergene B. And Yalçın B., "Finite element analyzing of the effect of crack on mechanical behavior of honeycomb and re-entrant structures", ***Politeknik Dergisi***, 23(4): 1015-1025, (2020).

Erişim linki (To link to this article): http://dergipark.org.tr/politeknik/archive

DOI: **10.2339/politeknik.534103**

Finite Element Analyzing of the Effect of Crack on Mechanical Behavior of Honeycomb and Reentrant Structures

Highlights

- *Regular honeycomb and re-entrant structures with rib thickness of 1mm, 1.5mm and 2mm were designed.*
- *The effect of presence of crack and crack propagation in these structures were investigated.*
- *Finite element analysis were examined by using Ansys Apdl.*
- *The effect of crack on stress intensity factor, stresses, strains and displacement were obtained.*

Graphical Abstract

The effect of crack on the mechanical behavior of honeycomb and reentrant structures was analyzed by using the finite element method. The results emphasize that the presence of crack influences the stress and displacements of cellular structures significantly.

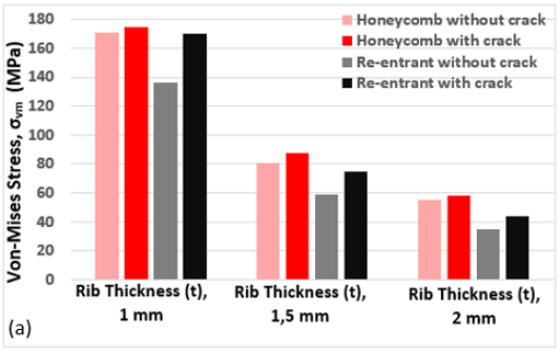

Figure. Equivalent stress (σ_{vm}) results

Aim

The effect of crack on stress, stress distribution and displacement of honeycomb and re-entrant structures were studied and its analyzed that in which cases the crack could advance or not.

Design & Methodology

Honeycomb structure with positive Poisson's ratio and re-entrant structure with negative Poisson's ratio were designed and subsequently analyzed with finite element method.

Originality

The effect of crack and crack propagation was examined in popular cellular structures which can be also additively manufactured.

Findings

The stress intensity factor (K_I) obtained from the FE analyses showed that increase in rib thickness provides decreasing the K_I values at crack tip. Increment in relative density increased the fracture toughness as well.

Conclusion

In this study, the crack propagation is expected only at honeycomb structure with t of 1 mm. Because the value of the stress intensity factor is greater than the fracture toughness.

Declaration of Ethical Standards

The authors of this article declare that the materials and methods used in this study do not require ethical committee permission and/or legal-special permission.

Finite Element Analyzing of the Effect of Crack on Mechanical Behavior of Honeycomb and Re-entrant Structures

Araştırma Makalesi / Research Article

Berkay ERGENE[1*], Bekir YALÇIN[2]

[1]Pamukkale University, Faculty of Technology, Department of Mechanical and Manufacturing Engineering, Turkey
[2]Isparta Applied Sciences University, Technology Faculty, Mechanical Engineering Department, Türkiye

(Geliş/Received : 01.03.2019 ; Kabul/Accepted : 02.10.2019)

ABSTRACT

Developments in technology require the new materials, lighter and more efficient structures and also new manufacturing methods. In this study, after doing researches about topology optimization, regular honeycomb and re-entrant structures; the regular honeycomb and re-entrant structures were designed, and then Ti-6Al-4V material was chosen for these structures in finite element (FE) analyzing. The three different rib thickness values (t) of 1 mm, 1.5 mm and 2 mm were assigned for honeycomb and re-entrant structures in FE analyses. Also, the crack was created on the models, and then 2-D FE analyses were done for both cracked and un-cracked honeycomb and re-entrant structures under tensile forces through y axis. Afterwards, the effect of crack on stress intensity factor, stresses, strains and displacement were obtained and characterized the auxetic behavior of the regular honeycomb and re-entrant structures. Furthermore, increase in rib thickness decreases stress and strains for each structure. Moreover, re-entrant structures have negative Poisson's ratio due to their geometric properties and the notable effect of crack on the equivalent stress in re-entrant was emerged in comparison with honeycomb structure. As a result, the only possible fracture in honeycomb for thickness of 1 mm might be observed owing to stress intensity factor obtained from analyses bigger than fracture toughness of honeycomb structure.

Keywords: Auxetic behavior, crack, negative Poisson's ratio, stress intensity factor.

Çatlağın Re-entrant ve Balpeteği Yapıların Mekanik Davranışlarına Etkisinin Sonlu Eleman Analizi

ÖZ

Teknolojideki gelişmeler yeni malzemeler, daha hafif ve daha verimli yapıları ve ayrıca yeni üretim yöntemlerini gerektirmektedir. Bu çalışmada, topoloji optimizasyonu, düzenli balpeteği yapıları ve re-entrant yapılar hakkında araştırmalar yapıldıktan sonra düzenli balpeteği ve re-entrant yapılar tasarlanmış ve sonrasında Ti6Al4V malzeme, sonlu elemanlar analizinde kullanılmak üzere seçilmiştir. Sonlu elemanlar analizlerinde balpeteği ve re-entrant yapılara 1 mm, 1,5 mm ve 2 mm olmak üzere üç farklı kiriş kalınlığı atanmıştır. Ayrıca, modellerde çatlak oluşturulmuş ve sonrasında 2 boyutlu sonlu elemanlar analizleri y ekseni boyunca uygulanan çekme kuvvetleri altında hem çatlaklı hem çatlaksız balpeteği ve re-entrant yapılar için yapılmıştır. Daha sonra, çatlağın gerilme yığılma faktörü, gerilmeler, gerinimler ve yer değiştirmelere etkileri elde edilmiş ve düzenli balpeteği yapıların ve re-entrant yapıların ökzetik davranışı karakterize edilmiştir. Ayrıca, her bir yapı için kiriş kalınlığındaki artış gerilme ve gerinimleri azaltmaktadır. Dahası, re-entrant yapılar geometrik özelliklerinden dolayı negatif poisson oranına sahiptirler ve çatlağın re-entrant yapıdaki eşdeğer gerilmeye etkisi balpeteği yapısına kıyasla dikkate değer bir şekilde ortaya çıkmaktadır. Sonuç olarak, sadece 1mm kiriş kalınlığına sahip balpeteği yapısında analizlerden elde edilen gerilme yığılma faktörünün balpeteği yapının kırılma tokluğundan büyük olmasından dolayı kırılma gözlemlenmesi beklenmektedir.

Anahtar Kelimeler: Ökzetik davranış, çatlak, negatif Poisson oranı, gerilme yığılma faktörü.

1. INTRODUCTION

Today, industrial firms are in competition to develop and manufacture specific products at a high level flexibility and quality, lighter, low cost and machining time. This competition reveals the new manufacturing method like additive manufacturing (AM) technologies and the new engineering materials and design like auxetic and foam structures for aircraft industry, automotive, medical, sports and leisure sectors.

Also, the first auxetic structure was introduced by Lakes [1] and these structures have potential applications such as sandwich panel cores, energy and sound damping, aerospace filler foams, radome frames, bioimplants, arterial prosthesis, composite tails, defense personal protective equipment, human wearing helmet, seat belts and safety harnesses etc. due to their unique properties such as energy absorption for crash and impact protection, and thermal transfer, excellent shear stiffness and strength, indentation resistance, high fracture toughness and low relative density [2-7]. Some of the

*Sorumlu Yazar (Corresponding Author)
e-posta : berkay_ergene@hotmail.com

applications for auxetic materials were tabulated in Table 1.

Table 1. Some applications for auxetic materials [8].

Field	Existing and potential applications
Aerospace	Vanes for gas turbine engines, thermal protection, aircraft nose cones, wing panel, sounds and vibrations absorber, rivet.
Automotive	Bumper, cushion, thermal protection, sounds and vibrations that need shear resistant, fastener.
Biomedical	Bandage, wound pressure pad, dental floss, artificial blood vessel, artificial skin, drug release unit, ligament anchors, surgical implants, similar to that of bone characteristic.
Composite	Fiber reinforced for reducing the cracking between fiber and matrix.
Military	Helmet, bullet proof vest, knee pad, glove, protective wear having better impact property.
Sensor/ actuators	Hydrophone, piezoelectric devices, various sensors having the low bulk modules which make them more sensitive to hydrostatic pressure.
Textile	Fibers, functional fabric, color change straps

One of the new class of engineering materials is auxetic material, providing the further advantages [2-7]. Generally, when the tensile force is applied to conventional structure in x axis direction, the shrinkage in the perpendicular direction (y axis) occurs at the structure according to elasticity theory. On the contrary, the auxetic structure exhibits expanding in perpendicular direction when load is applied to the structure in horizontal direction (x axis). So, the expression of negative Poisson's ratio in the auxetic structure has been emerged [8].

It is known that many properties depend on the Poisson's ratio of the material from classical elasticity theory. So, the shear modulus (G) and the bulk modulus (K) are obtained with well-known Eq. (1 and 2).

$$G = \frac{E}{2(1+\nu)} \tag{1}$$

$$K = \frac{E}{3(1-2\nu)} \tag{2}$$

Where, E and ν are the Young's modulus and Poisson's ratio, respectively. According to continuum mechanics, K is named as bulk module which determines most materials resist a change in volume; G determines most materials resist a change in shape [8].

It can clearly be seen from Eq. (1) that when ν approaches to −1, which is the limit for an isotropic material, the shear modulus will become infinitely. Also, when this tendency approaches to infinite extremes as $\nu \rightarrow -1$, the properties such as indentation resistance, thermal shock resistance, and fracture toughness have been improved. Thus, auxetic materials show certain enhanced properties because of their negative Poisson's ratio [9]. Eq. (3) is obtained by combining the Eq. (1 and 2), so the materials can be classified with respect of Poisson's ratio (Fig. 1).

$$\left(\frac{1+\nu}{1-2\nu}\right) \geq \frac{3}{2} \tag{3}$$

According to Eq. (3), Poisson's ratio of conventional materials can't be less than 0.125. When the Poisson's ratio value is less than zero, the bulk modulus must be much less than shear modulus. Eq. (4) is obtained by combining the Eq. (1 and 2), and then Poisson's ratio can be obtained with Eq. (5) [8].

$$\left(\frac{1+\nu}{1-2\nu}\right) \geq \frac{3K}{2G} \tag{4}$$

$$\nu = \left(\frac{3K-2G\nu}{2G-6K}\right) \tag{5}$$

A material having negative Poisson's ratio is known as auxetic material, shown in Fig. 1. Generally, while conventional honeycomb structures expand with compression loads, re-entrant structures expand in all directions under the tensile loads, as shown in Fig. 2-a and 2-b. Therefore, the re-entrant auxetic structure will have a negative Poisson's ratio close to – 1, and by this way, this structure gains the higher shear stiffness, strength, damping capacity, indentation resistance and fracture toughness.

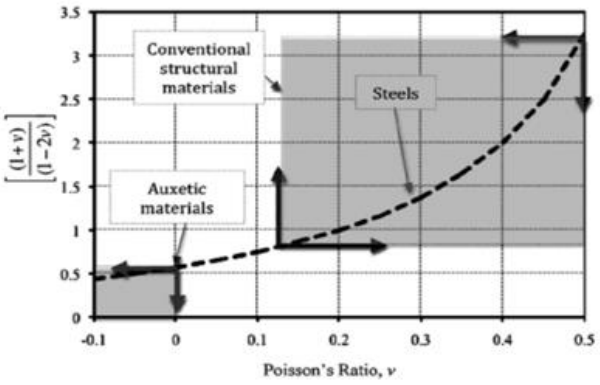

Figure 1. The relation between the Poisson's ratio and the value of y axis for conventional and auxetic materials [8].

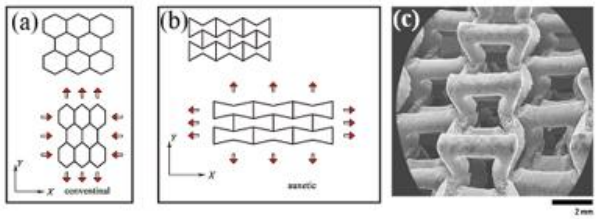

Figure 2. a) Non auxetic conventional honeycomb structure with positive Poisson's ratio, b) Re-entrant auxetic structure with negative Poisson's ratio [10], c) Re-entrant auxetic structure by 3D printing [11].

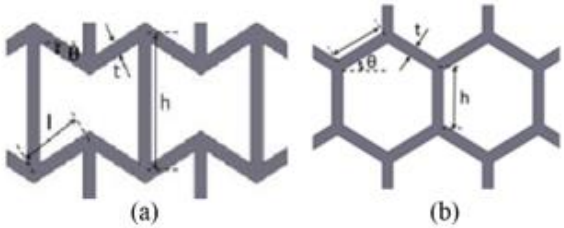

Figure 3. a) The dimensional definition for re-entrant auxetic structure, b) for conventional honeycomb structure

To understand the mechanical and fracture behavior of auxetic structure, its fracture mechanic has to be comprehended. In this context; the fracture mechanic formulas of any auxetic structure are as follows;

According to Maiti et al. [12]; works; stress intensity factor (KI) is,

$$\sigma = \left(\frac{(K_I)}{\sqrt{2\pi r}}\right) + \left(\frac{(K_I)}{\sqrt{2\pi r}}\right)\left(\frac{(r_{tip})}{2r}\right) \tag{6}$$

Where, K_I is stress intensity factor, rtip is crack tip radius, $r>r_{tip}$. The force acting on each cell rib;

$$F = \int_{r_{\frac{tip}{2}}}^{r_{\frac{tip}{2}+1}} \left[\frac{(K_I)}{\sqrt{2\pi r}} + \frac{(K_I)}{\sqrt{2\pi r}}\left(\frac{r_{tip}}{2}\right)\right] r_{tip}\partial r \tag{7}$$

In Eq. (7), t is the thickness of rib, Also, Green [13] developed an equation for cellular material semi-empirical, can be seen in Eq. (8).

$$\frac{K_{IC}}{\sigma_f\sqrt{\pi l}} = 0.28\left(\frac{\rho}{\rho_s}\right)^{1.3} \tag{8}$$

Where, K_{IC} is the fracture toughness of cellular material, σf is the failure stress. It can be seen in Fig. 3 that l is the length of cell rib, ρ is the density of cellular material, ρ_s is the density of solid material [13]. Moreover, similar fracture toughness for the re-entrant auxetic structure was given in Eq. (9) [14];

$$\frac{K_{IC}}{\sigma_f\sqrt{\pi l}} = 0.1\left(\sqrt{\frac{1+\sin\left(\frac{\pi}{2}-\theta\right)}{1+\cos^2\theta}}\,\frac{\rho}{\rho_s}\right) \tag{9}$$

K_{IC} is the fracture toughness for the re-entrant auxetic structure and θ is the rib angle in Eq. (9). Moreover, the elasticity modulus changes with a change in the density of materials. Therefore, the density and elasticity modulus of auxetic structure were respectively calculated with Eq. (10 and 11) depending on the solid material. According to the accepted mechanic of auxetic structure, the density (ρ) and elasticity modulus (E_y) were followed [15, 16];

$$\left(\frac{\rho}{\rho_s}\right) = \frac{\frac{t}{l}\left(\frac{h}{l}+2\right)}{2\cos\theta\left(\frac{h}{l}+\sin\theta\right)} \tag{10}$$

$$E_y = \left(\frac{\left(\frac{h}{l}-\cos\theta\right)}{2\frac{h}{l}l^2\sin^2\theta + \frac{l^4}{2E_s t^4} + \frac{3l^2}{2G_s t^2}\sin^4\theta}\right) \tag{11}$$

In Eq. (11), E_s and G_s are the elasticity and shear modulus of solid materials. It can be seen from Eq. (6-11) that the performance of auxetic structure could be largely affected by its geometric properties such as cellular shape, rib thickness and angle, relative density together with cellular material and manufacturing method.

When the cell is the regular hexagons, then then θ=30° and h=l, the relative density is that [17];

$$\left(\frac{\rho}{\rho_s}\right) = \left(\frac{2}{\sqrt{3}}\frac{t}{l}\right) \tag{12}$$

Where, t is rib thickness, h and l are length of rib for cell of regular honeycomb in Eq. (12). The elasticity modulus of regular honeycomb through y axis (E_y) can be obtained by the following Eq. (13). E_s is the elasticity modulus of solid material [17]. In addition, the fracture toughness ($K_{ıc}$) of regular honeycomb structure was expressed in Eq. (14).

$$\left(\frac{E_y}{E_s}\right) = \frac{4}{\sqrt{3}}\left(\frac{t}{l}\right)^3 \tag{13}$$

$$K_{IC} = 0.3\sigma_f\sqrt{\pi l}\left(\frac{t}{l}\right)^2 \tag{14}$$

Ability to manufacture the various porous and auxetic structure designs from different materials with AM methods have been investigated in the literature. For example, any auxetic structure was designed with the following topology optimization steps: the determining the forces exposed to structure, the calculation of effective structure properties, converge of structure optimization, the determining the structure shape sensitive to forces and optimization the structure [18].

In new one [19], plastic analyses on re-entrant and non-entrant thin walled steel honeycombs structure were carried out. They impressed that the re-entrant has better energy absorption than the honeycomb. Yang et al. [15] investigated on compressive properties of Ti–6Al–4V auxetic mesh structures made by electron beam melting (EBM). A Ti–6Al–4V 3-D re-entrant lattice auxetic structure having two relative density and two Poisson's ratios were manufactured by EBM, and then compressive tests were performed in their work. They impressed that re-entrant lattice structure has superior mechanical properties compared to regular foam structures. Ingrole et al. [16] realized on design and modeling of auxetic and hybrid honeycomb structures for in-plane property enhancement. They reported that the new design of auxetic structure has 65% high compressive strength than the re-entrant auxetic structure and 300% more than that of honeycomb structure. Besides, Bates et al. [20] manufactured the honeycomb structures from polyurethane with fused filament method which is one of the AM methods, and then the energy absorption behavior of all structures was experimentally investigated. Their research demonstrated the potential for 3D printed, hyperplastic honeycombs as energy absorbing structures, with the structures created meeting the criteria of resiliency, good energy absorbing efficiency and quality of manufacture. Carneiro et al. [21] also reported that, the auxetic structures have a superior capacity of acoustic absorption than conventional honeycomb structure. Argatov et al. [22] noted that the auxetic materials have an improved indentation

resistance, when compared to conventional materials. Moreover, Bianchi et al. [23] mentioned that, the auxetic structure can be reverted to conventional honeycomb structure several times without loss of mechanical characteristics at desirable temperatures. Also, Yalçın and Ergene [24] analyzed the effect of crack on mechanical behavior of hybrid composites and presented that the shear stresses increase with increasing the crack angle. Additionally, Akkuş et al. [25] investigated the mechanical behavior of aluminum honeycomb structures under compression with experimental and finite element methods. They found 85% accuracy between experimental and analysis results.

In this study, the auxetic behavior is primarily determined for conventional honeycomb and re-entrant structures with FE analyses. Secondly, the cracks on each cellular structure were formed and then vertical tensile force was applied through y axis to crack. The cellular material constants such as elasticity modulus and Poisson's ratio were calculated by using Eq. (10-13) with respect of solid Ti-6Al-4V material constants and auxetic mechanic in FE analyses. The stress intensity factor (K_I), the normal stresses (σ_x and σ_y), von Mises stresses (σ_{vm}), shear stresses (τ_{xy}), displacement values (Δl_x and Δl_y) and stress concentrations on the cell rib were obtained from the analyses. The results of stress, strain, displacement and Poisson's for regular honeycomb and re-entrant structures were interpreted.

2. MATERIALS AND METHOD

2.1 Finite Elements Modelling Procedure

After doing literature survey [10, 11, 16 and 25], the honeycomb and re-entrant structures were designed with engineering design program and then these models were exported to the finite element based program (ANSYS). Models were created as with and without crack and also three different rib thicknesses of 1 mm, 1.5 mm and 2 mm were assigned for each honeycomb and re-entrant structures. Also, length of rib (l), height of rib (h) and rib angle (θ) is 5.2 mm, 5.2 mm and 30°, respectively. In re-entrant structure, l, h and θ are respectively followed as 5 mm, 10 mm and 30°.

The cracks on FE models were located to left of structures. The materials of re-entrant and honeycomb structures were chosen as Ti-6Al-4V which has elasticity modulus (E) of 114000 MPa, Poisson's ratio (ν) of 0,342 and density (ρ) of 4,43 g/cm^3. Subsequently, the FE models were homogeneously meshed with element type Quad 4 node 42 and optimized. Also, the bottom of model was fixed as ancastre; the tensile stress of 2 MPa was applied to top of the structures by applying 5000N to all nodes at the top of the structure (Fig. 4g). FE models and the cracked model were show in Fig. 4. Then, 2-D FE analyses option were carried out in ANSYS program by using selected element type's plane stress with thickness input option.

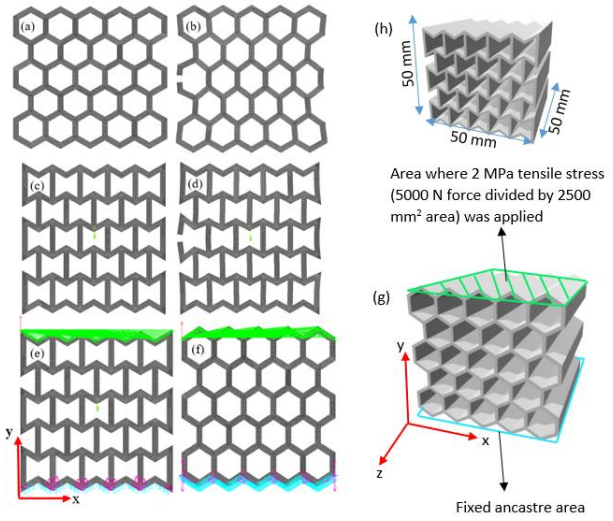

Figure 4. Finite element models a) un-cracked honeycomb, b) cracked honeycomb, c) un-cracked re-entrant, d) cracked re-entrant, e) boundary conditions on re-entrant, f) boundary conditions on honeycomb, g) view of boundary conditions on 3D model, h) dimensions of the models.

Afterwards, σ_x, σ_y, τ_{xy}, σ_{vm}, Δl_x, Δl_y and stress concentrations on the cell rib were obtained from the analyses. Moreover, stress intensity factor of K_I was obtained from analyses. The results of stress and strain for conventional honeycomb and re-entrant auxetic structures were interpreted with respect of stress concentrations, the effect of crack on the K_I, σ_x, σ_y, σ_{vm}, τ_{xy}, Δl_x, Δl_y and Poisson's ratio. Moreover, stress intensity factors in crack tip of K_I were achieved for each structure in FE analysis. Fig. 5 shows the selected nodes on path to calculate K_I values. It is known that K_I significantly determines the possible crack advance with effect of stresses on structure.

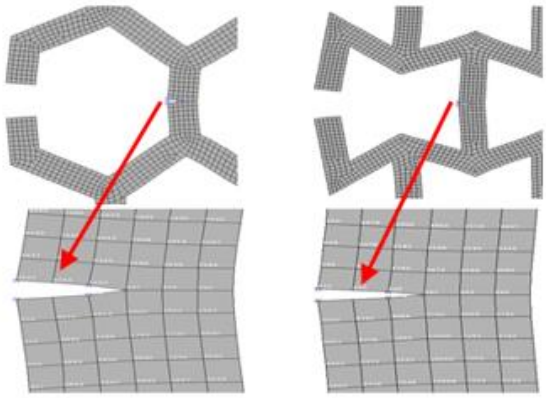

Figure 5. The selected nodes on path to calculate K_I values

3. RESULTS

3.1 Stress Results and Auxetic Behaviour

Fig.6-a and Fig 6-b present normal stresses in x and y axes for honeycomb and re-entrant structures. According to Fig. 6-a, the lowest stress of max σ_x occurs on the un-

cracked re-entrant structure, and the highest max σ_x happens on the un-cracked honeycomb structure for t of 1 mm. Also, when rib thickness (t) is 2 mm, the most σ_x consisted in the cracked honeycomb structure. The max σx in un-cracked honeycomb for rib thickness of 1 mm is 11.4 % more than that of the cracked honeycomb structure.

On the other hand, the max σ_x in un-cracked re-entrant for rib thickness of 1 mm is 19.6 % lower than that of the cracked honeycomb structure. As can be seen Fig 6-a, decreasing trend in the normal stresses through x axis were observed for all structures from FE analyses. For instance, when t increases from 1 mm to 2 mm for un-cracked honeycomb structure, the max σ_x decreases from 172.84 MPa to 46.45 MPa for un-cracked honeycomb, σx decreases from 153.78 MPa to 51.62 MPa for cracked honeycomb, and also max σ_x decreases from 123.73 MPa to 33.77 MPa for un-cracked re-entrant structure, in addition, max σ_x decreases from 149.02 MPa to 42.58 MPa for cracked re-entrant structure, respectively.

Moreover, the max σ_x in honeycomb structure occurred as compression; on the other hand, the max σ_x in re-entrant structure eventuated as tension. This state can be shown in Fig. 7 for un-cracked and cracked structures, t of 2 mm. This is very important results that while the maximum stresses through x axis cause shrinkage of the honeycomb structure and leads expansion of the re-entrant structure through x axis. This result gives information that the re-entrant structure shows exhibiting the auxetic behavior. Screenshots from FE analyses about expansion of the re-entrant structure for t of 1 mm and the shrinkage of honeycomb structure for t of 1 mm under tensile forces applied in y direction which were respectively shown in Fig 8-a and Fig 8-b.

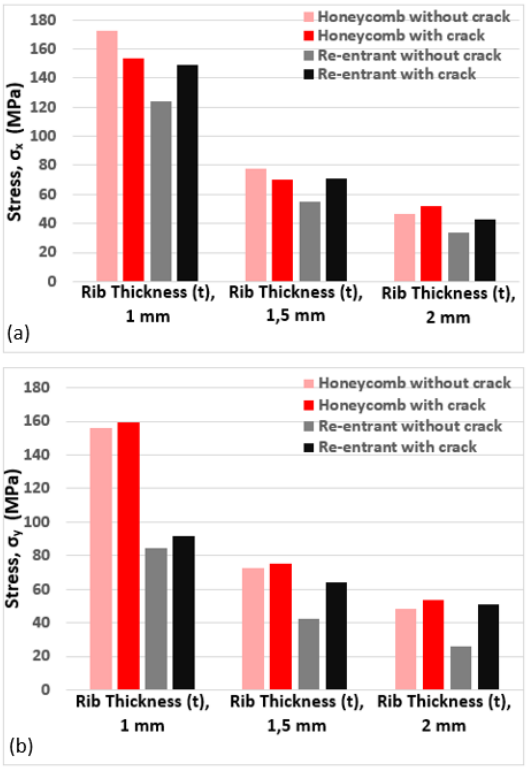

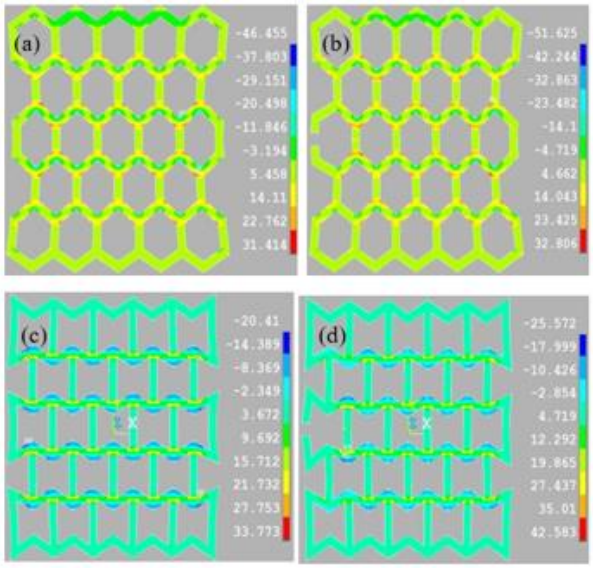

Figure 6. The max σ_x (a) and max σ_y (b) values obtained from FE analysis.

Figure 7. The maximum tension of σ_x in a) un-cracked and b) cracked honeycomb and the maximum compression of σ_x , c) in un-cracked and d) cracked re-entrant for 2 mm thickness.

Figure 8. Screenshots from FE analyses about, a) re-entrant structure expansion, b) the shrinkage of honeycomb structure under tensile loads.

According to the Fig 8, while the re-entrant structure possessing t of 1 mm, 1.5 mm, 2 mm expanded through x axis as 5.122 mm, 0.333 mm and 0.038 mm; the honeycomb structures for t of 1 mm, 1.5 mm, 2 mm shortened through x axis as 4.1 mm, 0.435 mm and 0.092 mm, respectively. Also, as rib thickness increased, the elongation and shortening values decreased for re-entrant and honeycomb structures, respectively. When evaluating the elongation and shrinkage values in x direction, the elongation for re-entrant for rib thickness of 1 mm is 19.95 % higher than shrinkage of honeycomb structure for thickness of 1 mm. However, as rib thickness increases, the auxetic behavior drops sharply owing to decrease in $\Delta lmax_x$ (expansion) in re-entrant

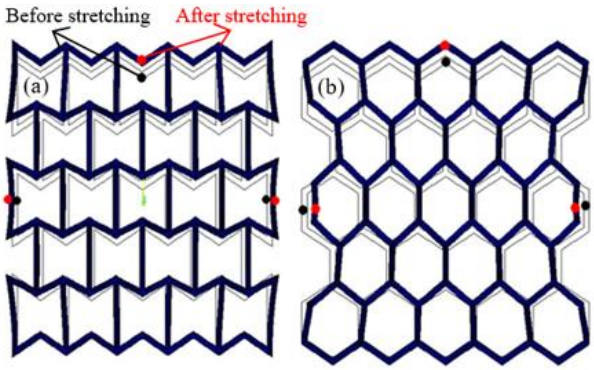

structure. For example, when rib thickness increases from 1 mm to 1.5 mm, the expansion of re-entrant trough x axis decreases from 5.122 mm to 0.333 mm. This result is important for topology optimization and to obtain the higher indentation resistance of any auxetic structure.

Table 2. The calculated constants for honeycomb and re-entrant structures

The calculated constants of the honeycomb structure				
Rib thickness (mm)	E (MPa)	ν	ρ (kg/mm^3)	Relative density (%)
1	1863.08	0.342	$9.83x10^{-7}$	22.18
1.5	6287.908	0.342	$14.74x10^{-7}$	33.27
2	14976.40	0.342	$19.66x10^{-7}$	44.37
The calculated constants of the re-entrant structure				
1	622.345	0.342	$13.64x10^{-7}$	30.79
1.5	2172.022	0.342	$20.46x10^{-7}$	46.18
2	4783.59	0.342	$27.28x10^{-7}$	61.58

The density (ρ) and elasticity modulus (E) values for the re-entrant and honeycomb structures in analyses were respectively calculated with Eq. (10-13), which were shown Table 2 and used in analysis. As can be seen Table 2, when rib thickness increases, the relative density increases. In this context, increase in relative density provides decreasing the normal stresses thorough x and y axes. Aslam et al. [26] reported that increasing of the relative density in auxetic structures decreases stresses in structure occurred under tension loads. Besides, the maximum stresses (σ_y) through y axis in each cracked structure are higher than those of each un-cracked structure. It is obvious that there is higher effect of crack on σy for re-entrant structure than that of honeycomb structure. Also, the crack of re-entrant structure for t of 1.5 mm and 2 mm has higher influence on σ_y when comparing the t of 1 mm. On the other hand, σ_y values in honeycomb linearly change; in addition, there is a linear effect of crack on σy values in honeycomb structure for all rib thicknesses. For example, when the rib thickness is 1 mm, the crack effect increased the σy 2.5%, for rib thickness of 1,5 mm 4% increment, and for rib thickness of 2 mm 9.4% increment observed on honeycomb structure. Also, as rib thickness is 1 mm, the crack effect increased the σ_y 8.5 %, for rib thickness of 1,5 mm 52% increment, and for rib thickness of 2 mm 93% increment observed on re-entrant structure. Ingrole et al. [16] showed that the absorption capacity of re-entrant structure is 19% more than honeycomb structure. Also, Scarpa and Smith [4] expressed auxetic structures possess energy and sound dampening. Equivalent stress (σ_{vm}) results were given in Fig. 9-a. As similar tendency was obtained from FE analyses about equivalent and shear stresses (Fig. 9a and Fig. 9b). The equivalent and shear stresses in un-cracked and cracked honeycomb structure are higher than those of in un-cracked and cracked re-entrant structure.

Generally, maximum σ_{vm} stress concentrated on the nearest rib and rib joint to crack in the cracked honeycomb and re-entrant structures, which were given in Fig. 10 for t of 1 mm. As can be seen in Fig 10, the maximum σ_{vm} didn't occur at the crack tip; however, at the top rib joint of the cracked cell exposed the maximum σ_{vm} of 174.595 MPa. Moreover, the maximum Von mises stress (σ_{vm}) of 169.966 MPa occurred on bottom rib joint of the cracked cell in re-entrant structure. As similar honeycomb, the maximum σ_{vm} did not occur at the crack tip of re-entrant structure.

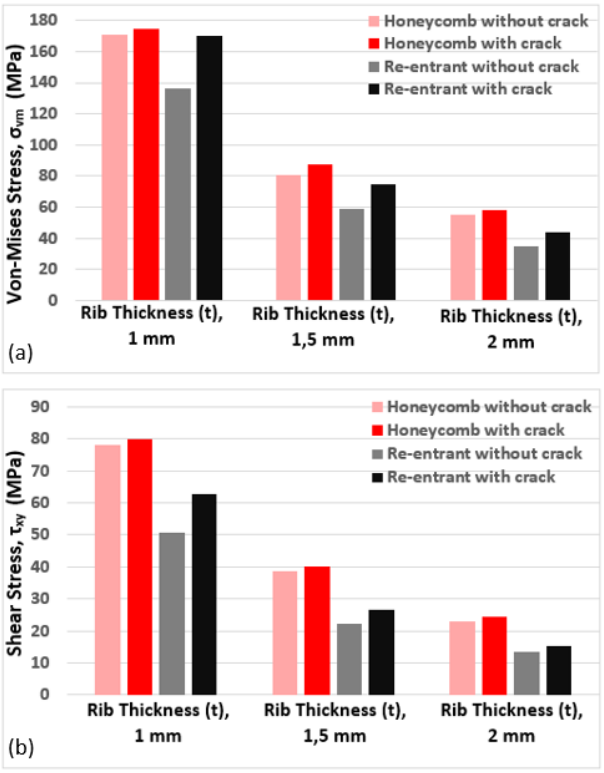

Figure 9. a) Equivalent stress (σ_{vm}) results, b) Shear stress (τ_{xy}) results

If Fig. 10 and Fig. 11 are examined, the σ_{vm} stresses change between 37.77 MPa and 56.655 MPa at the crack tip of re-entrant, between 38.799 MPa and 58.198 MPa at the crack tip of honeycomb structure. These values decrease with an increase in rib thickness. It is known that the stresses extremely increase at crack tip in homogeneous materials as different from foam structures [27]. Also, the maximum stresses concentrated at the crack tip leads advancing the crack when stress intensity factor (K_I) equals or higher than the fracture toughness (K_{IC}) of the material. Moreover, in homogeneous materials, the possible crack starts from the crack tip lay on continuous patch in literature [27]. As can be seen in Fig. 10 and Fig. 11 that the crack propagation in foam structures such as re-entrant and honeycomb are lower than homogeneous materials due to fact that the maximum stresses did not enforce to the crack tip. Therefore, the possible crack advance doesn't occur on the continuous patch. Fleck et al. [28] mentioned that the crack propagation in foam structure doesn't lie on continuous patch, but the crack advances on sinuous patch. Also, they impressed that the crack growth behavior depends on the cell wall materials and geometric properties of honeycomb structures. The maximum stresses at crack tip of re-entrant structure are lower than those of honeycomb in this FE analysis, which

can be seen in Fig.10 and Fig. 11. Therefore, it is conceivable that the crack advance in re-entrant structure may lower than that of honeycomb structure. Ravirala, et al. [29] reported that the crack resistance to fracture of re-entrant structure is higher than non-auxetic structure like honeycomb.

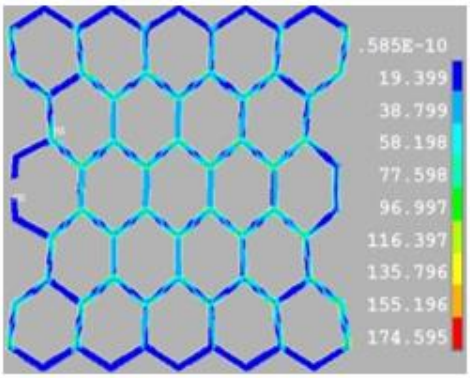

Figure 10. σ_{vm} stress distributions in cracked honeycomb structure

In the context of this study, the fracture toughness values for re-entrant and honeycomb structures were respectively calculated with Eq. 9 and 14. Besides, the stress intensity factor values (K_I) at crack tip were obtained from FE analyses, which can be seen in Table 3. According to the fracture mechanics [27], when $K_I=K_{IC}$, the fracture takes place and leads to the crack propagation. According to Table 3, stress intensity factors obtained from the FE analyses showed that the increase in rib thickness provides the decrease of Kı values at crack tip. Also, when rib thickness increases, relative density increase, which can be seen in Table 2.

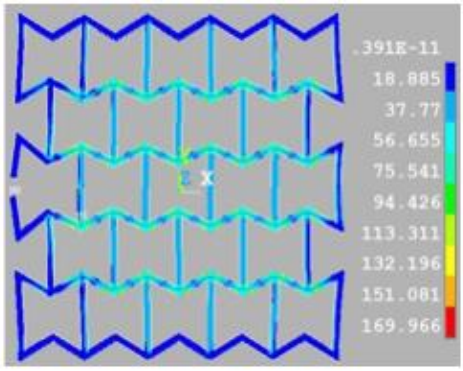

Figure 11. σ_{vm} stress distributions in cracked re-entrant structure

Table 3. K_I values obtained from FE Analyses and the calculated K_{IC} values with Eq. (9, 14)

t (mm)	Honeycomb Structure		Re-entrant Structure	
	Obtained K_I from FEA (MPa√m)	Calculated K_{IC} by formulas (MPa√m)	Obtained K_I from FEA (MPa√m)	Calculated K_{IC} by formulas (MPa√m)
1	64,392	38,634	51,608	82,086
1.5	48,823	86,930	44,168	123,130
2	41,666	154,544	39,870	164,173

According to the fracture mechanics, if the stress intensity factor equals ($K_I=K_{IC}$) or higher than fracture toughness, the fracture resistant decreases, fracture starts in structure, and crack propagation goes on [27]. Otherwise, when the obtained stress intensity factor value is lower than fracture toughness, the crack doesn't advance or occur in un-crack structure. If this situation is commented, crack propagation in honeycomb structure with t of 1 mm will be expected due to fact that its stress intensity factor value is higher than its fracture toughness. On the other hand, the crack in re-entrant structure doesn't advance because of the stress intensity factor is lower than its fracture toughness (Table 3). It means that the re-entrant structure possesses resistant to fracture more than honeycomb structure. Furthermore, it doesn't seem the crack propagation in rest of cracked honeycomb and re-entrant structures for the reason of much less stress intensity factor value than the calculated fracture toughness values. Rehme et al. [30] expressed that the fracture toughness of the re-entrant open-cell copper sponge is 1.5 times of the fracture toughness value of conventional open-cell copper sponge. As an example, from this study, the calculated fracture toughness of re-entrant structure and honeycomb structure for rib thickness of 1.5 mm is 123,130 MPa√m and 86,930 MPa√m respectively so fracture toughness of re-entrant structure is found 1.4 times of the fracture toughness of honeycomb structure. Also, the stress intensity factor in crack tip of re-entrant structure is 8.3 % lower than that of honeycomb structure.

3.2 Strain and Displacement Results

In order to better characterize the behavior of re-entrant and honeycomb structures, displacement, strain and Poisson's ratio values were respectively shown in Fig. 12, Fig. 13 and Fig 15. Fig. 12 presents the maximum displacement values of Δl_x and Δl_y through x and y axes, respectively. The most important result was obtained from analyses that while the maximum shrinkage ($-\Delta lmax_x$) in honeycomb structure occurred, the maximum expansion ($+\Delta lmax_x$) took place in re-entrant structure through x axis under tension loads through y axis, which can obviously be seen in Fig. 12-a. This result exhibits the auxetic behavior of re-entrant structure. Especially, in case of rib thickness decreasing to 1 mm, more expansion through x axis occurred than other rib thicknesses of re-entrant structure. The effect of crack on shrinkage through x axis in honeycomb structure is less than the effect of crack on expansion in re-entrant structure. Also, the maximum elongation ($+\Delta lmax_y$) was observed for each structure under tension loads through y axis. This state can be seen in Fig 12-b. Moreover, the maximum Δl_y values of re-entrant structure are higher than those of honeycomb structure. The reason of this phenomena can be explained that the re-entrant structure possesses less elasticity modulus than honeycomb structure. In addition, high movement ability of angled struts in re-entrant structure through y axis and the effect of this movement to vertical struts lead to have more displacement on y axis.

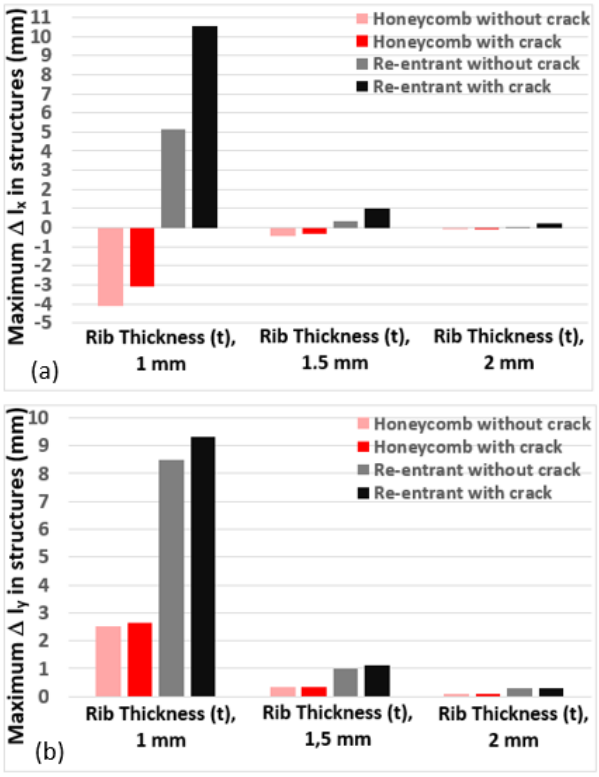

Figure 12. a) Maximum displacement through x axis, Δl_x
b) maximum displacement through y axis, Δl_y

Fig. 13 presents maximum strains through x and y axis for each structure. It is mainly known that the strain is the ratio of dimensional change to initial size ($\Delta l/L_o$). So, a similar tendency in strains was obtained with displacement values. As can be seen in Fig 13, decrease in rib thickness cause increasing the strain values. The maximum strain of εmaxx ($+\Delta l max_x/L_x$) in re-entrant structure gets positive value because of the elongation in x axis different from honeycomb structure. On the other hand, the negative maximum strains ($-\Delta l max_x/L_x$) through x axis in honeycomb structure were obtained due to shrinkage on x axis. Also, when rib thickness is 1 mm, the evident increment in max ε_x observed for each re-entrant and honeycomb structure. Also, maximum strains of εmaxy ($+\Delta l max_y/L_y$) in both re-entrant and honeycomb structures get positive values because of the elongation behavior in y axis under stretch through y axis. It is known that some materials properties such as shear and bulk modulus depend on Poisson's ratio (ν). The Poisson's ratio of the honeycomb and re-entrant structures were determined by Gibson and Ashby theory [31] which is accepted to determine for cellular structure. As similar, Joseph et al. [32] expressed that Poisson's ratio can be calculated with determining the ε_x and ε_y in the group of centermost cells instead of εmax_x and εmax_y in honeycomb and re-entrant structures. The reason selection this centermost cell to determine Poisson ratio is attempting to minimize edge effect. In this study, the Poisson ratio was determined according to the accepted theory [31, 32].

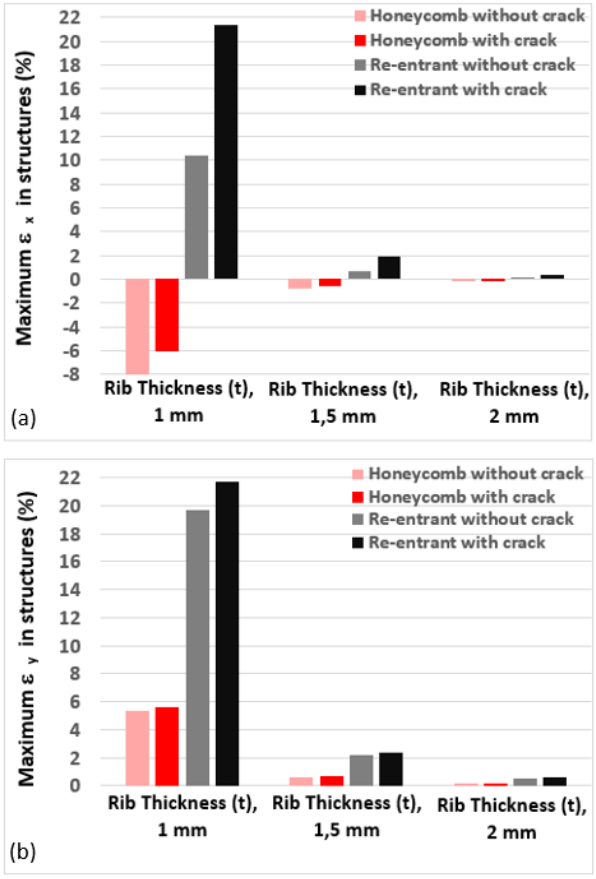

Figure 13. a) Maximum strain values through x axis, ε_x
b) maximum strain values through y axis, ε_y

Fig. 14 shows the method of calculating Poisson's ration and definition on key points used to determine ε_x and ε_y for centermost cell. According to the accepted theory to determine the Poisson's ratio, ε_x values were calculated with displacement values on **.1** nodes through x axis in group of centermost cells for each structure, in addition, ε_y values were calculated with displacement values on **.2** nodes through y axis in group of centermost cells for each structure.

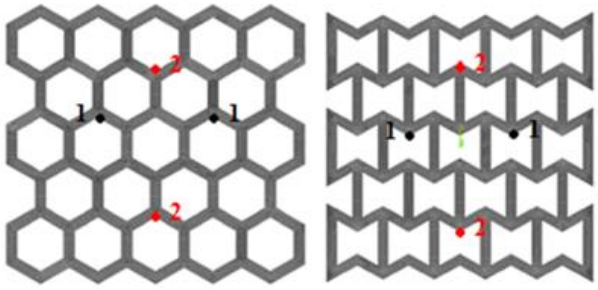

Figure 14. Definition of key points to determine the Poisson's ratio in FE analyses

The obtained Poisson's ratio as $\longrightarrow \nu = -(\varepsilon_x/\varepsilon_y)$ from FE analyses were given in Fig. 15. As can be seen in Fig 15, the re-entrant structure possess negative Poisson's ratio due to expansion in x axis; while the positive Poisson's ratio obtained due to happening the shrinkage through x axis in honeycomb structure when stretching,

Therefore, the re-entrant structures exhibits auxetic behavior because of possess the negative Poisson's ratio with expansion in x direction under scratching through y axis. Moreover, re-entrant structures having negative Poisson's ratio can be recommended in applications required the indentation resistant and absorption. Because, although the re-entrant structure has the low elasticity modulus, it shows conducting the low stress concentrations, high strain values, and the expansion through x axis under tension load applied in y direction. Because of auxetic behavior in re-entrant structure, high indentation resistant was observed from FE analyses.

Recent studies showed that these structures attract attention of researchers and industrial company. For instance, Joseph et al. [32] compared the Poisson's ratio values of honeycomb and re-entrant structures, experimentally. They found the negative Poisson's ratio for re-entrant structure and positive Poisson's ratio for honeycomb structure in case of stretch in y direction. It can be obviously seen in their study, the Poisson's ratio values in honeycomb can be bigger than 1, and also the Poisson's ratio values in re-entrant can be bigger than -1 depending on rib length and height.

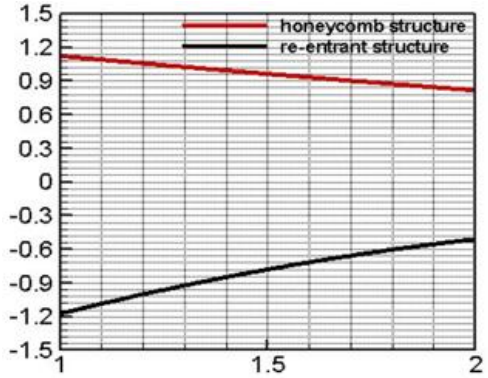

Figure 15. Poisson's ratio of honeycomb and re-entrant structures, ν

Furthermore, Osama et al. [33] reported that when the porosity of the cellular structure increases depending on decrease of strut thickness, Poisson's ratio value of honeycomb and re-entrant structure approaches to 1 and -1 from absolute lower values respectively. Lee et al. [34] expressed that Poisson's ratio of the regular honeycomb structure decreased when volume fraction increased. Moreover, Whitty et al. [35] emphasized about changing the rib thickness leads to a change in the Poisson's ratio for honeycomb and re-entrant structures. Greaves et al. [36] emphasized that for the future, the numerical metric that Poisson's ratio provides will be advantageous in researching and developing new materials, marrying the mechanical response of diverse components, from the nano to the macro scale through variable changes in shape and volume.

4. CONCLUSIONS

It is obviously understood that the modern structure was designed by topology optimization possessing more efficient, low density, high absorber capacity, indentation resistant and shear strength for specific industrial applications. Nowadays, they have been also manufactured by additive manufacturing methods. So, in order to estimate the effect of crack on mechanical and auxetic behaviors for regular honeycomb and re-entrant structures from Ti-6Al-V materials, FE analyses were realized with respect of the accepted auxetic mechanic in this search. In the literature, investigations focus on mechanical behavior of these materials under compression load. Likewise, Ergene and Yalçın conducted some studies [37, 38] to determine the compression behavior of honeycomb and re-entrant structures. On the other hand, as different from other researches, the mechanical behavior of honeycomb and re-entrant structures were analyzed under tensile force through y direction in this study. We have presented that increase in the rib thickness rises to the relative density for each structure. Besides, the re-entrant structure possesses much less relative density than honeycomb structure. Also, the fracture toughness values of both structures according to formula of the accepted cellular solid mechanic theory [11-19] were calculated. The K_{IC} of re-entrant structure is greater than that of honeycomb structure, and K_{IC} values are getting higher while increasing the rib thickness. Moreover, following are the major conclusion of this study;

- Firstly, increment in rib thickness decrease stresses and strains for each structure.
- The maximum σ_x in honeycomb structure occurred as compression; on the other hand, the max σ_x in re-entrant structure occurred as tension. This phenomenon causes expansion in re-entrant structure and leads shrinkage in honeycomb structure through x axis (Fig. 8).
- The crack increase in y direction stresses (σ_y) values comparing the un-cracked honeycomb and re-entrant structure; much less σ_y consisted in un-cracked re-entrant structure than honeycomb structure.
- The equivalent stresses (σ_{vm}) in re-entrant structure obtained lower than those of honeycomb structure. The notable effect of crack on stress σ_{vm} in re-entrant revealed in comparison with honeycomb structure. For example, increment ratio in von-Mises stress were respectively obtained as 6.89% and 22.97% with the effect of crack in honeycomb and re-entrant structures. Maximum σ_{vm} mostly concentrated on the closest rib joint of cracked cell for each structure.
- The stress intensity factor (K_I) obtained from the FE analyses showed that increase in rib thickness provides decreasing the K_I values at crack tip. Increment in relative density increased the fracture toughness.
- In the literature [28], if $K_I=K_{IC}$ equal or greater than fracture toughness, the crack resistance decreases, the fracture in structure starts and crack propagation continues. In this study, the crack propagation in honeycomb structure with t of 1 mm will be expected because the value of the stress intensity factor is greater than the fracture toughness. The crack propagation is

not expected in the rest of cracked honeycomb and re-entrant structures, because the stress intensity factor is less than the calculated fracture toughness.

- From the FE analyses, it is observed that the re-entrant structure possesses negative Poisson's ratio although honeycomb structure exhibits positive Poisson's ratio (Fig. 15).

Nomenclature

E_y : Elasticity modulus through y axis of auxetic structure
E_s : Elasticity modulus of solid material
G_s : Shear modulus of solid material
K_{IC} : Fracture toughness of auxetic structure
K_I : Intensity factor
θ : Rib angle
t : Rib thickness
F : The force acting on each cell rib
σ_f : Fracture strength
ρ_s : Density of solid material
ρ : Density of auxetic structure
L : Rib length
ν : Poisson's ratio
K : Bulk modulus

DECLARATION OF ETHICAL STANDARDS

The author(s) of this article declare that the materials and methods used in this study do not require ethical committee permission and/or legal-special permission..

REFERENCES

[1] Lakes R., "Foam structures with a negative Poisson's ratios", ***Science***, 235:1038–1040, (1987)

[2] Undershill R.S., "Defense applications of auxetic materials", ***Advanced Materials***, 1(1):7-12, (2014)

[3] Novak N., Vesenjak M., Ren Z, "Auxetic cellular materials - a review", ***Journal of Mechanical Engineering***, 62(9): 485-493, (2016)

[4] Scarpa F., Smith F.C., "Passive and MR fluid-coated auxetic PU foam –mechanical, acoustic, and electromagnetic properties***", Int. Journal Mater. Syst. Struct***., 15: 973–979, (2004)

[5] Yang L., Harrysson O., West H., Cormier D., "Mechanical properties of 3D re-entrant honeycomb auxetic structures realized via additive manufacturing", ***Int. Journal of Solids and Structures***, 69–70: 475–490, (2015)

[6] Choy Y.S., Sun C.N., Leonga K.F., Weia J., "Compressive properties of Ti-6Al-4V lattice structures fabricated by selective laser melting: Design, orientation and density", ***Additive Manufacturing***, 16: 213–224, (2017)

[7] Yan C., Hao L., Hussein A., Young P., Raymont D., "Advanced lightweight 316Lstainless steel cellular lattice structures fabricated via selective laser melting", ***Materials&Design***, 55: 533–541, (2014)

[8] Prawota Y., "***Solid Mechanics for Materials Engineers: Auxetic Materials Seen from the Mechanics Point of View***", Chapter 15, USA (2013).

[9] Alderson A., and Alderson K.L., "Auxetic materials", ***Journal of Aerospace Engineering***, 221 G: 565-575, (2007)

[10] Budarapu P.R., Sudhir Sastry Y.B., Natarajan R., "Design concepts of an aircraft wing: composite and morphing airfoil with auxetic structures", ***Front. Struct. Civ. Eng***., 10(4): 394–408, (2016)

[11] Critchley R., Corni I., Wharton J.A., Walsh F.C., Wood R.J.K., Stokes K.R., "The preparation of auxetic foams by three-dimensional printing and their characteristics", ***Adv. Eng. Mat***., 15 (10): 980–985, (2013)

[12] Maiti K., Ashby M.F., Gibson L.J., "Fracture toughness of brittle cellular solids", ***Scripta Metallurgica***, 18: 213-217, (1984)

[13] Green D., "Fabrication and mechanical properties of lightweight ceramics produced by sintering of hollow spheres", ***Journal of Am. Ceram. Soc***., 68: 403–409, (1985)

[14] Choi J., and Lakes R, "Fracture toughness of re-entrant foam materials with a negative Poisson's ratio: Experiment and analysis", ***Int. Journal of Fracture***, 80: 73–83, (1986)

[15] Yang L., Harrysson O., West H., Cormier D., "Compressive properties of Ti–6Al–4V auxetic mesh structures made by electron beam melting", ***Acta Materialia***, 60: 3370–3379, (2012)

[16] Ingrole A., Hao A., Liang R., "Design and modeling of auxetic and hybrid honeycomb structures for in-plane property enhancement", ***Materials & Design***, 117: 72–83, (2017)

[17] http://www.mse.mtu.edu/~drjohn/my4150/honey/h1.html

[18] Vogiatzis P., Chen S., "Topology optimization of 3d auxetic meta materials using reconciled level-set method", ***Proceedings of the ASME International Design Engineering Technical Conferences and Computers and Information in Engineering Conference***, USA (1986).

[19] Zhou Z., Zhou J., Fan H., "Plastic analyses of thin-walled steel honeycombs with re-entrant deformation style", ***Materials Science & Engineering***, A 688: 123–133, (2017)

[20] Bates S.R.G, Farrow I.R., Trask R.S, "3D printed polyurethane honeycombs for repeated tailored energy absorption", ***Materials &Design***, 112: 172–183, (2016)

[21] Carneıro V.H., Meıreles J., Puga H., "Auxetic materials – a review", ***Materials Science-Poland***, 31(4): 561-571, (2013)

[22] Argatov I.I., Diaz R.G., Sabina F.J., "On local indentation and impact compliance of isotropic auxetic materials from the continuum mechanics viewpoint", ***Int. Journal of Engineering Science***, 54: 42-57, (2012)

[23] Bianchi M., Scarpa F., Smith C.W., "Shape memory behaviour in auxetic foams: Mechanical properties", ***Acta Materilia***, 58: 858–865, (2010)

[24] Yalçın B., and Ergene B., "Analyzing the effect of crack in different hybrid composite materials on mechanical behaviors", ***Pamukkale University Journal of Engineering Sciences***, 24(4): 616-625, (2018)

[25] Akkuş H., Düzcükoğlu H., and Şahin Ö.S., "Experimental research and use of finite elements method on mechanical behaviors of honeycomb structures assembled with

epoxy-based adhesives reinforced with nanoparticles", ***Journal of Mechanical Science and Technology***,31(1): 165-170, (2017)

[26] Usman Aslam M., Darwish S.M., "Development and analysis of different density auxetic cellular structures", ***Int. Journal on Recent and Innovation Trends in Computing and Communication***, 3(1): 27-32, (2015)

[27] Hertzberg R.W., "***Deformation and Facture Mechanics of Engineering Materials***", 3. Edition, John Wiley, USA, (1989)

[28] Schmidt I., Fleck N.C., "Ductile fracture of two dimensional cellular structures", ***International Journal of Fracture***, 111: 324-342, (2001)

[29] Ravirala N., Alderson A, Alderson K, and Davies P., "Auxetic polypropylene films", ***Polym. Eng. and Sci***., 45: 517-528, (2005)

[30] Rehme O., Emmelmann C., "Selective laser melting of honeycombs with negative poisson's ratio", ***Journal of Laser Micro/Nanoengineering***, 4(2): 128-134, (2009)

[31] Gibson L.J., Ashby M.F., Schajer G.S., Robertson C.I., ***Proc. R. Soc. Lond***. A, 382, 25, (1982)

[32] Joseph N.G., Oliveri L., Attard D., Ellul B., Gatt R., Cicala G. and Recca G., "Hexagonal honeycombs with zero poisson's ratios and enhanced stiffness", ***Advanced Engıneerıng Materıals***, 12(9): 855-862, (2010)

[33] Osama A.M.A, and Darwish S.M.H., "Analysis, fabrication and a biomedical application of auxetic cellular structures", ***International Journal of Engineering and Innovative Technology***, 2(3): (2012)

[34] Lee J., Choi J.B., and Choi K., "Application of homogenization FEM analysis to regular and re-entrant honeycomb structures", ***Journal of Materials Science***, 31: 4105- 4110, (1996)

[35] Whitty J.P.M., Nazare F., and Alderson A., "Modelling the effects of density variations on the in-plane poisson's ratios and young's moduli of periodic conventional and re-entrant honeycombs - part 1: Rib thickness variations", ***Cellular Polymers***, 21(2): 69-98, (2005)

[36] Greaves G.N., Greer A.L., Lakes R.S., and Rouxel T., "Poisson's ratio and modern materials", ***Nature Materials***, 10: 823-838, (2011)

[37] Ergene B., Yalçın B., "Finite element analysis for compression behaviour of polymer based honeycomb and re-entrant structures", 4th International Conference on Engineering and Natural Sciences, 549-556, 2-4 May, Kiev-Ukraine, 2018.

[38] Yalçın B., Ergene B., Karakılınç U., "Modal and stress analysis of cellular structures produced with additive manufacturing by finite element analysis (FEA)", ***6th International Symposium on Innovative Technologies in Engineering and Science***, 263-272, 9-11 November, Antalya-Turkey, 2018